Annals of Botany **116**: 713–725, 2015
doi:10.1093/aob/mcv094, available online at www.aob.oxfordjournals.org

ANNALS OF BOTANY
Founded 1887

PART OF A SPECIAL ISSUE ON REACTIVE OXYGEN AND NITROGEN SPECIES

Site-directed mutagenesis substituting cysteine for serine in 2-Cys peroxiredoxin (2-Cys Prx A) of *Arabidopsis thaliana* effectively improves its peroxidase and chaperone functions

Eun Mi Lee[1,†], Seung Sik Lee[1,†], Bhumi Nath Tripathi[1], Hyun Suk Jung[2], Guang Ping Cao[3], Yuno Lee[3], Sudhir Singh[1], Sung Hyun Hong[1], Keun Woo Lee[3], Sang Yeol Lee[3], Jae-Young Cho[4] and Byung Yeoup Chung[1,*]

[1]Advanced Radiation Technology Institute, Korea Atomic Energy Research Institute, 29 Geumgu-gil, Jeongeup 580-185, Republic of Korea, [2]Department of Biochemistry, College of Natural Sciences, Kangwon National University, Chuncheon 200-701, Republic of Korea, [3]Division of Applied Life Science (BK21 Program), Systems and Synthetic Agrobiotech Center (SSAC), Plant Molecular Biology and Biotechnology Research Center (PMBBRC), Research Institute of Natural Science (RINS), Gyeongsang National University, 501 Jinju-daero, Jinju 660-701, Republic of Korea and [4]Department of Bioenvironmental Chemistry, Chonbuk National University, Jeonju 561-756, Republic of Korea
** For correspondence. E-mail bychung@kaeri.re.kr*
† These authors contributed equally to this work.

Received: 27 February 2015 Returned for revision: 23 March 2015 Accepted: 8 May 2015 Published electronically: 2 July 2015

• **Background and Aims** The 2-Cys peroxiredoxin (Prx) A protein of *Arabidopsis thaliana* performs the dual functions of a peroxidase and a molecular chaperone depending on its conformation and the metabolic conditions. However, the precise mechanism responsible for the functional switching of 2-Cys Prx A is poorly known. This study examines various serine-to-cysteine substitutions on α-helix regions of 2-Cys Prx A in Arabidopsis mutants and the effects they have on the dual function of the protein.
• **Methods** Various mutants of 2-Cys Prx A were generated by replacing serine (Ser) with cysteine (Cys) at different locations by site-directed mutagenesis. The mutants were then over-expressed in *Escherichia coli*. The purified protein was further analysed by size exclusion chromatography, polyacrylamide gel electrophoresis, circular dichroism spectroscopy and transmission electron microscopy (TEM) and image analysis. Peroxidase activity, molecular chaperone activity and hydrophobicity of the proteins were also determined. Molecular modelling analysis was performed in order to demonstrate the relationship between mutation positions and switching of 2-Cys Prx A activity.
• **Key Results** Replacement of Ser^{150} with Cys^{150} led to a marked increase in holdase chaperone and peroxidase activities of 2-Cys Prx A, which was associated with a change in the structure of an important domain of the protein. Molecular modelling demonstrated the relationship between mutation positions and the switching of 2-Cys Prx A activity. Examination of the α_2 helix, dimer–dimer interface and C-term loop indicated that the peroxidase function is associated with a fully folded α_2 helix and easy formation of a stable reduced decamer, while a more flexible C-term loop makes the chaperone function less likely.
• **Conclusions** Substitution of Cys for Ser at amino acid location 150 of the α-helix of 2-Cys Prx A regulates/enhances the dual enzymatic functions of the 2-Cys Prx A protein. If confirmed *in planta*, this leads to the potential for it to be used to maximize the functional utility of 2-Cys Prx A protein for improved metabolic functions and stress resistance in plants.

Key words: *Arabidopsis thaliana*, chaperone, 2-Cys peroxiredoxin, 2-Cys Prx A protein, homology modelling, molecular dynamics simulation, peroxidase, reactive oxygen species, ROS, site-directed mutagenesis.

INTRODUCTION

Peroxiredoxins (Prxs) are ubiquitous thiol-based peroxidases capable of reducing a broad range of toxic peroxides and peroxinitrites in almost all living organisms (Tripathi *et al*., 2009; Dietz, 2011). Based on their subunit composition and position and the number of conserved cysteine (Cys) residues, Prx can be divided into the four sub-classes 1-Cys Prx, 2-Cys Prx, Prx II and Prx Q (Bhatt and Tripathi, 2011). Distinct locations, transcriptional regulation and structural and functional variations of Prx suggest specific biological roles of these sub-classes of Prx in the plant cell (Park *et al*., 2000; Dietz, 2003). Among these sub-classes, 2-Cys Prx has received greater attention due to its capability to act as chaperone, protein-binding partner, enzyme activator and redox sensor, along with its peroxide detoxification property (Muthuramalingam *et al*., 2009).

2 Plant 2-Cys Prx is nuclear-encoded but exclusively located in chloroplasts, the most active site of the redox metabolism in plant cells (Baier and Dietz, 1997). Two isoforms of 2-Cys Prx, *viz*. 2-Cys Prx A and 2-Cys Prx B, have been identified in *Arabidopsis thaliana* (Kirchsteiger *et al*., 2009) and account for ∼0·6 % of total chloroplast protein (Baier *et al*., 1996; Baier and Dietz, 1996). Although 2-Cys Prx is an obligate

homodimer, it frequently changes its conformation (reduced dimer, reduced oligomer, oxidized dimer and hyperoxidized dimer) depending on the redox status (Muthuramalingam *et al*., 2009). 2-Cys Prx is considered a functional hub in redox-dependent regulation and signalling in the chloroplast (Bhatt and Tripathi, 2011). Earlier studies suggested a protective role of 2-Cys Prx in chloroplasts against oxidative damage by inactivation and regulation of H_2O_2 at an optimal level. Suppression of 2-Cys Prx A has been shown to impair photosynthetic capacity in plants and increase the susceptibility of chloroplast proteins to oxidative damage (Baier and Dietz, 1999; Baier *et al*., 2000). Pulido *et al*. (2010) have demonstrated altered redox homeostasis and a marked increase in H_2O_2 content in chloroplasts of *A. thaliana* 2-Cys Prx A-2-Cys Prx B (Δ2cp) double mutants. Furthermore, over-expression of 2-Cys Prx increased tolerance of heat and oxidative stresses in tall fescue and potato plants (Kim *et al*., 2010, 2011) and increased the tolerance of reactive nitrogen species in yeast cells (Sakamoto *et al*., 2003).

3 Peroxide released during oxidative stress causes hyperoxidation of 2-Cys Prx, leading to a reversible conformational change from a low molecular weight (LMW) form to a high molecular weight (HMW) form (Muthuramalingam *et al*., 2009). However, this conformational change impairs the peroxidase activity of 2-Cys Prx (predominantly in the LMW form), but enables 2-Cys Prx to act as a molecular chaperone to prevent misfolding or aggregation of intracellular macromolecules caused by stress (Chuang *et al*., 2006). The chaperone function of 2-Cys Prx has already been established in bacteria (Chuang *et al*., 2006), yeast (Jang *et al*., 2004) and mammalian cells (Yang *et al*., 2002) and has subsequently been reported from the plant kingdom (Tripathi *et al*., 2009). It has been reported that 2-Cys Prx efficiently prevents the heat-dependent aggregation of citrate synthase and reduction-dependent aggregation of insulin (Jang *et al*., 2004; Kim *et al*., 2009; Muthuramalingam *et al*., 2009; An *et al*., 2010, 2011*a*). Thus, depending on its conformation, 2-Cys Prx may function as a peroxidase or molecular chaperone to protect the plant cell from either oxidative damage or denaturation or aggregation of intracellular proteins during stress conditions (König *et al*., 2013). The dual functions of these proteins are associated with dynamic reversible changes in their quaternary structure and also depend on the oxidation of peroxidatic Cys (C_p), phosphorylation, oxidative and/or heat stress, irradiation, etc., which induce a structural change in 2-Cys Prx from the LMW to the HMW form (König *et al*., 2013). Based on this description, it is assumed that 2-Cys Prx evolved as a multi-functional protein that switches between a high-affinity but low-turnover peroxidase function and a low-affinity but high-turnover chaperone function (König *et al*., 2013).

4 The enhancement of one of these activities (peroxidase and chaperone) of 2-Cys Prx may be an effective strategy to harness the potential of these molecules to the greatest advantage. However, earlier attempts to manipulate 2-Cys Prx to enhance one of these activities have compromised the efficiency of the other activity (An *et al*., 2011*a*; Hong *et al*., 2012). Recently, however, Park *et al*. (2014) have reported that proton irradiation can enhance both the peroxidase and the chaperone activity of PaPrx (2-Cys Prx). It has also been observed that the dual function of 2-Cys Prx can be regulated by an additional Cys on the α-helix region between two active Cys residues (An *et al*., 2011*b*). The presence of additional Cys residues promotes the oligomerization of 2-Cys Prx from the LMW form to the HMV form and thereby affects the switching of this protein between the two physiological functions. Therefore, further research is warranted to get better insight into the regulation and improvement of the dual function of 2-Cys Prx.

5 Based on the above, the present study investigated: (1) the production of various Ser → Cys substituted mutants of 2-Cys Prx A; (2) the regulatory mechanism of 2-Cys Prx A and in turn ways of enhancing its dual functions; and (3) the role of helix formation in Bas1 using molecular dynamics (MD) simulation studies for improvement of the two activities.

In the molecular modelling part of this study, we focused on observing the structural differences between wild-type (WT) 2-Cys Prx A and six mutants developed by point mutation (substitution of Cys for Ser) at residues 127, 131, 150, 180, 182 and 219. Wild-type 2-Cys Prx A had low chaperone and peroxidase activities, and in this it differed from six of the 2-Cys Prx A mutants, which demonstrated better chaperone or peroxidase activity. Mutants S127C, S131C and S150C showed high chaperone activity and S150C, S180C and S182C showed high peroxidase activity. However, S219C showed low chaperone and peroxidase activity. Hence, an investigation to identify the protein structural changes responsible for improvement in these activities was performed, employing the molecular modelling approaches of homology modelling and MD simulation.

MATERIALS AND METHODS

Site-directed mutagenesis of 2-Cys Prx A and protein expression

A cDNA of *Arabidopsis thaliana* encoding 2-Cys Prx A was cloned following standard procedures and was used to generate the mutants S127C, S131C, S150C, S180C, S182C and S219C by substituting Cys for Ser^{127}, Ser^{131}, Ser^{150}, Ser^{180}, Ser^{182} and Ser^{219}, respectively, by PCR-mediated site-directed mutagenesis. 2-Cys Prx A and all mutants were subsequently cloned in pGEM-T Easy vector (Promega, Madison, USA) and the point mutations were verified by automated DNA sequencing.

We cloned 2-Cys Prx A and its mutants in pET28a(+) expression vector (Novagen, Madison, USA), subsequently transformed and over-expressed in *Escherichia coli*. Then, His-tagged protein was purified from *E. coli* KRX (Promega) as described by An *et al*. (2010). In brief, 2 L of LB medium containing 50 μg ml^{-1} kanamycin was inoculated with 20 ml of a non-induced overnight bacterial culture and was grown to optical density (OD_{600}) 0·6 at 37 °C. Expression of recombinant protein was induced by adding L-rhamnose monohydrate to a final concentration of 0·2 % (w/v) at 30 °C. After 3 h, the cell pellet obtained by centrifugation (Supra 22k, Hanil, Korea) at 4000 *g* for 20 min was resuspended in lysis buffer (50 mM Na_2HPO_4, 500 mM NaCl, pH 8·0) and stored at –20 °C until used. For protein purification, the cell suspension was sonicated (VCX500, Sonics, USA) at an amplitude of 23 % on ice for 15 min intermittently. The cell debris was removed by spinning at 7000 *g* for 20 min at 4 °C. The soluble crude protein extract was loaded onto a nickel nitrilotriacetate agarose column (Peptron, Daejeon, Korea), previously equilibrated with five column volumes of phosphate-buffered saline (PBS). The

protein was eluted with 150 mM imidazole in PBS and the protein-containing fraction was pooled and dialysed three times against 10 mM Tris–HCl (pH 7·4) for 3 h. Protein concentrations were determined with the Bio-Rad protein assay using bovine serum albumin as a reference.

Size exclusion chromatography and polyacrylamide gel electrophoresis

Protein size determination and purification of 2-Cys Prx A and its mutants was performed by fast protein liquid chromatography (FPLC; AKTA, Amersham Biosciences, Uppsala, Sweden) using a Superdex 200 HR 10/300 GL column (Amersham Biosciences) following a method described earlier (An *et al*., 2011*a*). The column was equilibrated and run with 50 mM Tris–HCl (pH 8·0) buffer containing 100 mM NaCl (0·5 ml min^{-1}). Fractions (F1, F2 and F3) with the desired protein were pooled, concentrated and used for further analysis. Sodium dodecyl sulphate–polyacrylamide gel electrophoresis (SDS–PAGE) under reducing or non-reducing conditions and native PAGE were performed as described previously (Moon *et al*., 2005).

Determination of peroxidase and molecular chaperone activity

The thioredoxin (Trx)-dependent peroxidase activity of the recombinant proteins of WT 2-Cys Prx A and its mutants was measured by monitoring NADPH oxidation in terms of the decrease in absorbance of the reaction mixture at 340 nm (An *et al*., 2011c). The recombinant protein was incubated in 50 mM HEPES (pH 8·0) containing 0·3 mM NADPH, 1·0 μM yeast Trx and 5·0 μM yeast Trx reductase at 30 °C for 5 min, followed by addition of 1·0 mM H_2O_2. Enzyme activity was recorded by measuring the change in absorbance at 340 nm for 10 min using a UV-visible spectrophotoscopy (Evolution 300 UV-Vis spectrophotometer; Thermo Scientific, Worcester, MA, USA). Then, the relative peroxidase activity of purified protein fractions (F1, F2 and F3) and the mutants (S127C, S131C, S150C, S180C, S182C and S219C) was also measured following the method described above. The relative peroxidase activities of the three fractions and the mutants of 2-Cys Prx A were calculated considering the peroxidase activity of total purified protein as 100 %.

Holdase chaperone activity was determined using malate dehydrogenase (MDH) as a heat-sensitive substrate. MDH was incubated in 50 mM HEPES buffer (pH 8·0) at 43 °C with various concentrations of recombinant proteins of 2-Cys Prx A and its mutants. Thermal aggregation of the substrate was estimated by monitoring the increase in turbidity at 340 nm for 15 min using an Evolution 300 spectrophotometer (Thermo Scientific) equipped with a thermostatic cell holder. Thermal aggregation of MDH without 2-Cys Prx A protein was considered as the control. Holdase activity of WT 2-Cys Prx A protein was determined at 1:1 and 1:3 molar ratio between substrate (MDH) and 2-Cys Prx A protein. The relative holdase chaperone activity of the three fractions and the mutants of 2-Cys Prx A was determined using same procedure as that described above. The relative holdase chaperone activities of three fractions and the mutants of 2-Cys Prx A were calculated considering the peroxidase activity of total purified protein as 100 %.

Foldase chaperone activity was analysed using 4 M guanidine hydrochloride-denatured glucose-6-phosphate dehydrogenase (G6PDH) as a substrate. Denatured G6PDH (2 μM) was diluted 50-fold in 50 mM Tris–HCl buffer (pH 7·5) containing 10 mM KCl, 2·5 mM $MgCl_2$ and 10 mM ATP, and refolding was monitored by assaying G6PDH activity (Hansen and Gafni, 1993). Foldase chaperone activity of WT 2-Cys Prx A was measured as percentage reactivation of G6PDH (calculated from native G6PDH) determined after incubation of the substrate with different concentrations of 2-Cys Prx A protein for 0, 1, 3, 6 and 24 h. Similarly, the relative foldase activity of the three fractions and the mutants was calculated considering the foldase activity of total purified 2-Cys Prx A protein as 100 %. In both cases, foldase 24 h activity was determined after incubation of the substrate with 5 μM of the respective proteins.

Measurement of hydrophobicity

The hydrophobicity of 2-Cys Prx A and its mutants was measured by examining the binding of 1,1′-bi(4-anilino)naphthalene-5,5′-disulphonic acid (bis-ANS; Invitrogen Corporation, Carlsbad, CA, USA) with protein in an assay mixture of 10 μM bis-ANS and 50 μM protein in 50 mM HEPES buffer (pH 8·0). Bis-ANS fluorescence excitation was set as 380 nm and emission was scanned between 400 and 600 nm using an Infinite M200 (Tecan Group, Männedorf, Switzerland) as described earlier (Sharma *et al*., 1998).

Transmission electron microscopy and image processing

Transmission electron microscopy (TEM) and image analysis were performed following the method described by Lee *et al*. (2009). Briefly, different molecular weight fractions of 2-Cys Prx A were applied to glow-discharged carbon-coated copper grids. After allowing the protein to absorb for 1–2 min, the grids were rinsed with deionized water and stained with 2 % uranyl acetate. For metal shadowing, proteins were mixed with an equal volume of glycerol and solution was sprayed onto freshly cleaved mica. Grids were examined in a Technai G2 Spirit Twin TEM (FEI, USA) operated at 120 kV at a magnification of 51 k. The electron microscopy methods used were as described by Burgess *et al*. (2004).

Circular dichroism spectroscopy

Circular dichroism (CD) spectral analysis of 10 μM purified proteins of WT 2-Cys Prx and its mutants in 100 mM potassium phosphate buffer (pH 8·0) and 5.0 mM NaCl was performed with a spectropolarimeter (J-715; Jasco, UK) using a modification of Reed's method (Reed and Reed, 1997). All spectra were collected and averaged at least three times from independent experiments.

Molecular modelling

Homologues of 2-Cys Prx A were identified by performing sequence database searches using standard tools, such as PSI-BLAST and blastp. Homology modelling was conducted to

construct the 3-D structure of 2-Cys Prx A. Haem-binding protein 23 (HBP23)/Prx I from *Rattus norvegicus* (PDB ID: 2Z9S) (Matsumura *et al*., 2008) was selected as a structural template to construct the reduced decamer. A 3-D model of 2-Cys Prx A was constructed using the MODELLER module in Discovery Studio (DS) 3.5 (Martí-Renom *et al*., 2000; Eswar *et al*., 2006). The structures were validated with the PROCHECK (Laskowski *et al*., 1993) program and ProSA-web (Wiederstein and Sippl, 2007) to evaluate stereochemical properties. Energy minimization was performed for refinement of the seven systems (WT and six mutants) using the Smart Minimizer algorithm implemented in DS 3.5. The active-site Cys^{119} (Cp) in each subunit was oxidized to Cys sulphenic acid (Cp-SOH) using the Vienna-PTM webserver (Margreitter *et al*., 2013) for all systems. In total, seven different MD simulations were performed using the GROMACS program (version 4.5.3) (Berendsen *et al*., 1995; Van der Spoel *et al*., 2010) with the GROMOS54A7 force field (Schmid *et al*., 2011). The modified structures were immersed in an orthorhombic water box (1·2 nm thickness) and the net charge was neutralized by the addition of Na^+ counter ions. The long-range electrostatic interactions were calculated by the particle mesh Ewald (PME) method (Darden *et al*, 1993). Constant pressure and temperature for the whole system (1 bar and 300 K) were achieved with a Parrinello-Rahman barostat (Parrinello and Rahman, 1981) and V-rescale thermostat (Bussi *et al*., 2007). Production runs (10 ns) were performed under periodic boundary conditions with an NPT ensemble. The time step for the simulations was set to 2 fs and the coordinate data were written to the file every 10 ps. All analyses of MD simulations were carried out with GROMACS and DS 3.5 software.

Statistical analyses

The relative peroxidase and chaperone activities of various fractions of the purified 2-Cys PrxA and of the mutated and wild 2-Cys Prx A proteins were statistically analysed by one-way ANOVA (SPSS version 16.0), followed by a multiple comparison of the mean values (presented in Figs 3 and 4) by Duncan's test ($P = 0.05$). The mean and standard error were calculated from triplicates ($n = 3$) from three independent experiments.

RESULTS

2-Cys Prx A functions as both a peroxidase and a molecular chaperone

Figure 1A shows the peroxidase activity of 2-Cys Prx A measured in terms of NADPH oxidation by H_2O_2. Peroxidase activity was high and concentration-dependent. 2-Cys Prx A also showed holdase chaperone activity. Increasing the concentration of 2-Cys Prx A in the assay mixture significantly prevented aggregation of the MDH substrate protein (Fig. 1B). Similarly, 2-Cys Prx A showed a concentration-dependent increase in foldase chaperone activity, as evident from the >70 % restoration of activity of denatured G6PDH (substrate) by 10 μM 2-Cys Prx A protein (Fig. 1C).

2-Cys Prx A exists in multiple oligomeric forms

Based on the analysis of molecular size of the purified fraction of 2-Cys Prx A by size exclusion chromatography (SEC),

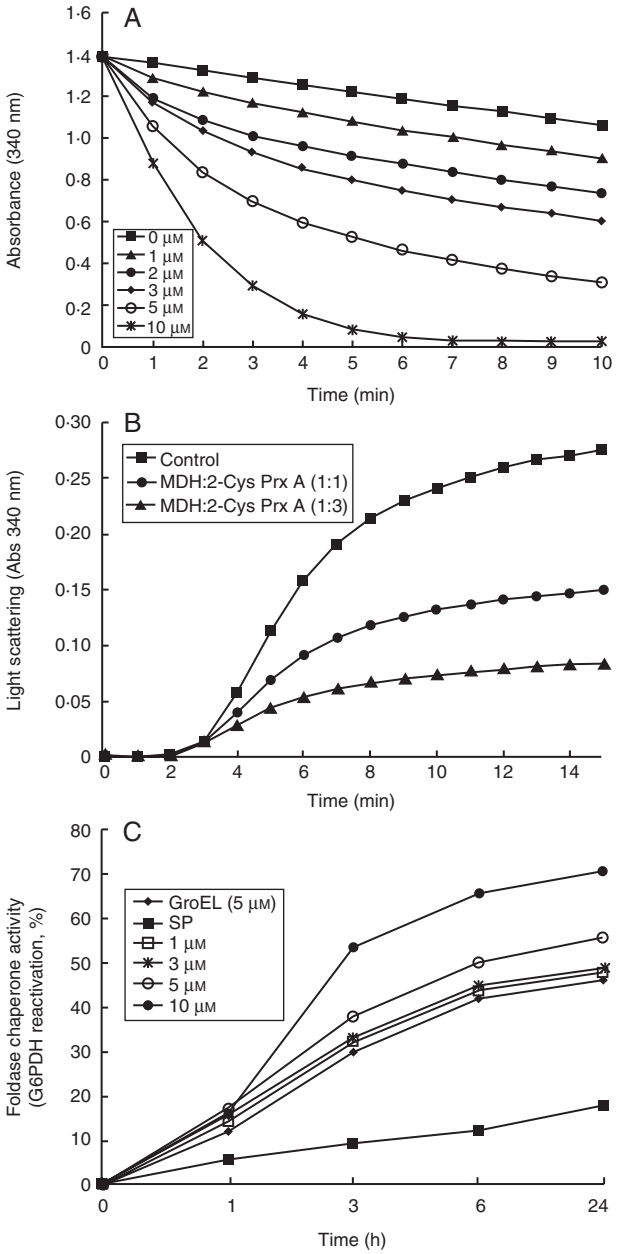

FIG. 1. (A) Peroxidase activity of WT 2-Cys Prx A measured in terms of NADPH oxidation. Curves of NADPH are shown for different concentrations of 2-Cys Prx A protein. Recombinant protein was incubated in 50 mM HEPES (pH 8.0) containing 0·3 mM NADPH, 1·0 μM yeast thioredoxin and 5·0 μM yeast thioredoxin reductase at 30 °C for 5 min, followed by addition of 1·0 mM H_2O_2. Enzyme activity was recorded by measuring the change in absorbance at 340 nm for 10 min. (B) Holdase chaperone function of WT-2-Cys Prx A was measured using MDH as substrate. Thermal aggregation curves are shown for 25 μg MDH incubated at 43 °C for 15 min. The control shows the thermal aggregation of MDH without 2-Cys Prx A. Holdase activity of 2-Cys Prx A was determined at 1:1 and 1:3 molar ratios between MDH and 2-Cys Prx A. (C) Foldase chaperone activity was measured using G6PDH as substrate. The cysteine-free form of G6PDH was denatured in guanidine–HCl and subsequently refolded in renaturation buffer in the presence of increasing concentrations of WT 2-Cys Prx A (1, 3, 5 and 10 μM). The refolding yield of G6PDH was determined by measuring G6PDH activity and expressed as a percentage of native G6PDH activity set to 100 %. GroEL indicates the activity of a standard chaperonin of *E. coli* and SP indicates the spontaneous reactivation of G6PDH without 2-Cys Prx A. Values are mean of three replicates ($n = 3$) with s.e. <3·0 % (not shown).

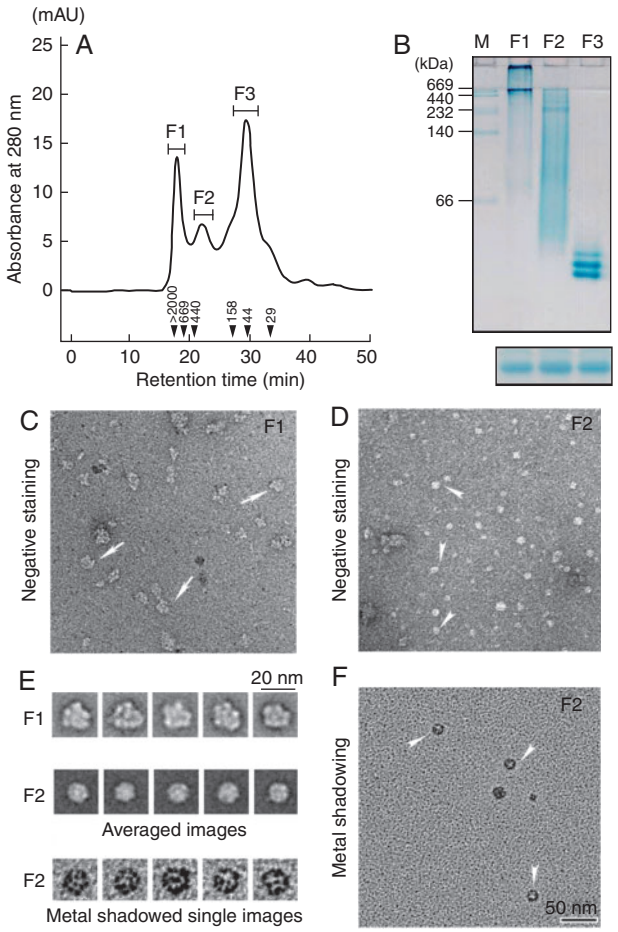

FIG. 2. (A) Protein structure of WT 2-Cys Prx A determined by SEC using a Superdex 200HR 10/30 column. The separated proteins were divided and pooled into three fractions (F1, F2 and F3; HMW complex, LMW complex and dimer, respectively). The numbers in the chromatogram represent the molecular weights of the standard proteins: blue dextran (>2000 kDa), thyroglobulin (669 kDa), ferritin (440 kDa), aldolase (158 kDa), ovalbumin (44 kDa) and carbonic anhydrase (29 kDa). (B) Structural analysis of fractionated 2-Cys Prx A protein by native PAGE. Each fraction was analysed by native PAGE (upper panel) or SDS–PAGE (lower panel) followed by Coomassie blue staining. (C–F) Electron micrographs of oligomeric complexes from WT 2-Cys Prx A. Negative staining of fraction F1 (HMW) and F2 (LMW) is shown in (C) and (D), respectively. (E) Averaged images of F1 and F2 and metal shadowing of F2 fraction. (F) Metal staining of fraction F2. White arrows and arrowheads (C, D, F) indicate individual particles found in the fields. Averaged images of F1 and F2 in (E) contain 20–40 particles.

three distinct forms – F1, F2 and F3 – were identified (Fig. 2A). Subsequen, native PAGE analysis showed that fraction F1, being an HMW complex, could not be resolved and thus was retained almost at the top of the separating gel (Fig. 2B). Fraction F2, an LMW complex, was present as an oligomeric complex of various sizes, whereas F3 exhibited a dimeric form (Fig. 2B). However, all three fractions showed a single band in SDS–PAGE analysis, with an apparent molecular weight of ~22 kDa (Fig. 2B, lower panel), suggesting that the 2-Cys Prx A protein forms a homo-oligomeric complex. A third, faint band appeared in the native gel of the dimeric form of F3 (Fig. 2B); the reason for this was unknown, but might be related to the presence of reduced, oxidized or over-oxidized forms of protein together in this fraction.

To further confirm the oligomeric status of 2-Cys Prx A, peak SEC fractions were examined by TEM. The electron micrograph of negatively-stained 2-Cys Prx A showed three different configurations. Fraction F1, corresponding to the HMW complex, was observed as spherical-shaped particles with a diameter of ~20 nm (Fig. 2C, E), whereas fraction F2 (LMW) was observed as a ring-shaped structure with size ranging from 14 to 16 nm (Fig. 2D–F). However, the protein in fraction F3 did not form any regular structure and therefore no image was taken.

Dual functions of 2-Cys Prx A are associated with its quaternary structure

The dual functions of a Prx are closely associated with its oligomeric status; hence, this relationship was explored by examining the peroxidase and molecular chaperone activities of the various fractions of 2-Cys Prx A protein obtained by SEC. The HMW complexes (F1) showed 4- to 5-fold higher holdase chaperone activity (Fig. 3B) but lower peroxidase activity (75 %) than that of total protein (Fig. 3A). In contrast, the F3 fraction exhibited ~1·5-fold higher peroxidase activity but 50 % lower holdase chaperone activity compared with total protein (Fig. 3A, B). The three fractions showed foldase chaperone activity similar to that of total protein (Fig. 3C). These results confirmed that the dual functions of 2-Cys Prx A are determined by its oligomeric status. Multimerization of 2-Cys Prx A enhanced its holdase chaperone activity, whereas dissociation promoted its peroxidase functions. Foldase chaperone activity appears to be associated with the concentration of 2-Cys Prx A rather than its conformational state.

Substitution with additional Cys residues in 2-Cys Prx A enhances its dual functions

In the present work, several mutants of 2-Cys Prx A were generated by replacing Ser with Cys in its crucial α-helix region. Among these mutants, S150C, S180C and S182C showed 3·6-, 2·6- and 2·7-fold, respectively, higher peroxidase activity compared with WT (Fig. 4A). Similarly, the holdase chaperone activity of S127C, S131C, S150C and S182C was 4·9-, 3·6-, 4·5- and 3·1-fold higher than that of WT (Fig. 4B). All the mutants except S127C showed similar or relatively better foldase chaperone (up to ~1·3-fold) activity compared with WT (Fig. 4C). Interestingly, S150C showed an increase in all three activities, suggesting that substitution of Cys for Ser at position 150 can play an important role in enhancing peroxidase and molecular chaperone functions.

To further investigate the structural changes in 2-Cys Prx A after addition of Cys, WT 2-Cys Prx A and mutants were analysed by SEC. The SEC results showed that WT and the mutants formed three different types of quaternary structure (Fig. 4D). S150C predominantly formed HMW and LMW complexes whereas S180C produced a dimeric form (Fig. 4D). S127C and S182C showed a pattern similar to that of WT. S180C was present mainly as a dimeric form, whereas S131C, and S127C, having a higher proportion of HMW complex, showed higher holdase chaperone activity. Mutants with a dimeric form showed higher peroxidase activity, but higher holdase chaperone activity was seen in the mutants with a higher proportion of HMW

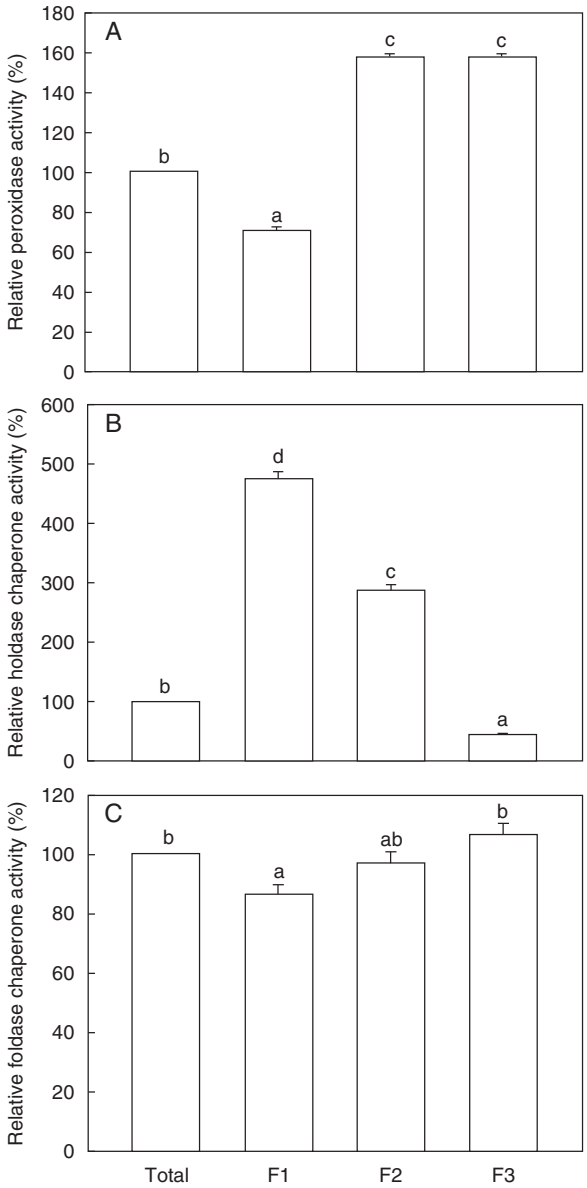

FIG. 3. (A) Relative peroxidase activities of fractionated 2-Cys Prx A protein. Activities of the three fractions were compared with that of total protein, which was set to 100 %. (B, C) Relative holdase (B) and foldase (C) chaperone activities of fractionated 2-Cys Prx A proteins. Activities of the three fractions were compared with activity of total protein, set at 100 %. Bars marked with different letters are significantly different from each other ($P < 0{\cdot}05$). Each data point is the mean ± s.e. of three replicates ($n = 3$) from three independent experiments.

complexes, indicating a relation between structure and function in these mutants. However, S150C, exceptionally, showed higher peroxidase and chaperone activity.

Ser → Cys substitution in 2-Cys Prx A leads to increased surface hydrophobicity and a change in structure

The interaction of non-native substrates with 2-Cys Prx A and its Cys-substituted mutants was confirmed using the fluorescent compound bis-ANS, which binds to hydrophobic patches of aminoacyl residues (Sharma *et al.*, 1998). Most 2-Cys Prx A mutants showed a significant increase in fluorescence intensity compared with WT, the maximum increase being shown by S150C (Fig. 5A). This suggests that Cys substitution led to an increase in exposure of hydrophobic patches of 2-Cys Prx A. However, S219C showed a decrease in hydrophobicity. These proteins showed a similar pattern of increase in their holdase chaperone activity (Fig. 4B). S150C, S131C, S182C and S127C, with relatively high increases in hydrophobicity, also showed better holdase chaperone activity. The increase in surface hydrophobicity is closely related to increased chaperone activity of proteins. These results suggest that additional Cys residues lead to exposure of more hydrophobic patches in 2-Cys Prx A mutants and in turn enhance holdase chaperone activity.

The influence of the replacement of Ser with Cys on the secondary structure of the protein was determined using UV–CD analysis. This analysis revealed the secondary structure of WT as 27·4 % α-helix, 51·2 % β-sheet and 24·4 % random coil without turn (Fig. 5B). The structures of S127C, S182C and S219C were almost similar to that of WT. However, in S150C the proportion of α-helix was markedly increased (to 71·2 %), with a concomitant decrease in the proportion of β-sheet (to 28·8 %). Interestingly, S131C and S180C proteins had completely lost their random coil segment.

Molecular modelling for the construction of 3-D structure of 2-Cys Prx A and correlation of structural differences with functional changes

A detailed atomistic molecular modelling study was undertaken to investigate the structure of 2-Cys Prx A and to find out why mutation leads to changes in structure and function. First, the 3-D structure of 2-Cys Prx A was constructed based on HBP23/Prx I from *R. norvegicus* (PDB ID: 2Z9S) (Matsumura *et al.*, 2008) (Fig. 6). The sequence of the 2-Cys Prx A protein shared ∼41·6 % sequence identity and 56·9 % sequence similarity with the template. The proportion of residues of 2-Cys Prx A in the most favoured regions was 91·2 %. The *Z*-score for WT 2-Cys Prx A (−6·83) was within the range of scores typically found for experimentally determined native proteins of similar size. Subsequently, C_P residues in the validated structures were modified to Cys sulphenic acid (C_P-SOH), considering the intermediate oxidation state. Six mutants (mutated from Ser to Cys at residues 127, 131, 150, 180, 182 and 219) were generated. The formation of inter-disulphide bonds in WT 2-Cys Prx A and six mutant systems were generated by linking the Cys residues and then conducting energy minimization.

In order to investigate the dynamic behaviour of these seven systems, 10-ns MD simulations were carried out with these four modified structures containing Cys sulphenic acid. The closest snapshot to an average structure over the last 1 ns of the trajectory was selected as a representative structure. The snapshots of WT 2-Cys Prx A (9680 ps), S127C (9130 ps), S131C (9560 ps), S150C (9600 ps), S180C (9570 ps), S182C (9070 ps) and S219C (9980 ps) were used to compare the protein structures between WT and mutant systems. S219C was not included in this study due to low chaperone and peroxidase activities.

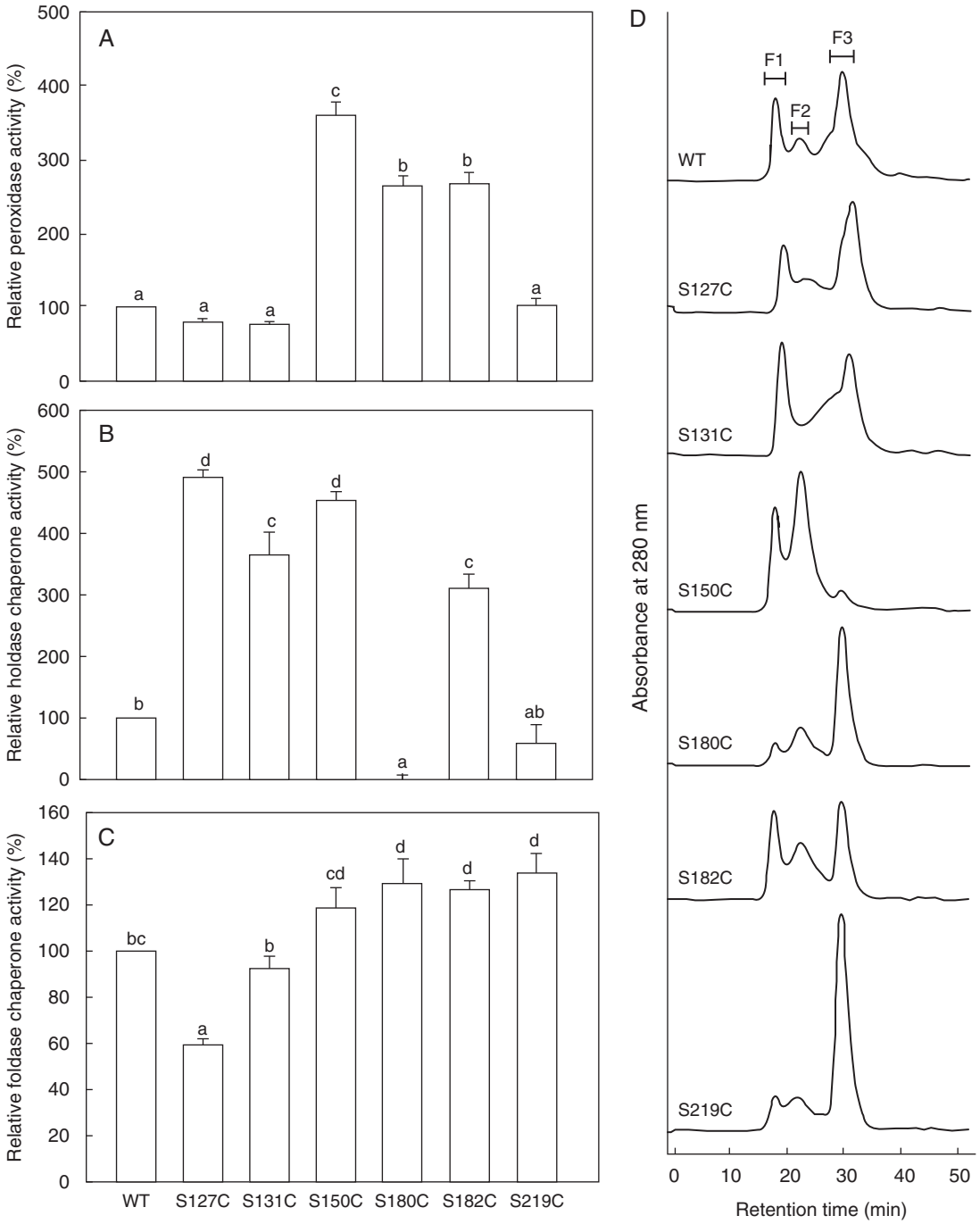

FIG. 4. (A) Relative peroxidase activities of Ser → Cys substituted 2-Cys Prx A mutants. The activities of the 2-Cys Prx A mutants were compared with that of WT 2-Cys Prx A, set at 100 %. (B, C) Relative holdase (B) and foldase (C) chaperone activities of point-mutated 2-Cys Prx As. Activities of 2-Cys Prx A mutants were compared with that of WT 2-Cys Prx A, set at 100 %. (D) Structural analyses of 2-Cys Prx A mutants by SEC. The six mutants of 2-Cys Prx A proteins (S127C-2-Cys Prx A, S131C-2-Cys Prx A, S150C-2-Cys Prx A, S180C-2-Cys Prx A, S182C-2-Cys Prx A and S219C-2-Cys Prx A) were separated by SEC and compared with WT 2-Cys Prx A. Proteins were divided into three fractions (F1, F2 and F3) by SEC, as shown in Fig. 2A. Bars marked with different letters are significantly different from each other ($P < 0{\cdot}05$). Each data point is the mean ± s.e. of three replicates ($n = 3$) from three independent experiments.

Peroxiredoxin exists as an obligate dimer that can form intermolecular disulphide bonds or remain in reduced form; the reduced and hyperoxidized dimeric structures have a strong tendency to form decamers or dodecamers (Barranco-Medina *et al*., 2009). Previous studies have suggested that the high molecular weight of typical 2-Cys Prx is related to chaperone activity, and hyperoxidation will induce oligomerization from the LMW to the HMW form, which assumes a chaperone function (Lim *et al*., 2008). The reduced form of 2-Cys Prx is fully folded in the HMW oligomerization process. Partial unfolding of the structure by movement of helix α_2 is needed to form the C_p-loop, to enable the peroxide substrate to oxidize the catalytic

site (C_p) (Barranco-Medina *et al.*, 2009). In other words, unfolding the α_2 helix will convert Prx to an oxidized decamer, which can increase the chaperone activity of Prx. Hence, α_2 helix structures of WT and three mutants (S127C, S131C and S150C) showing high chaperone activity were examined (Fig. 7). Residues 127 and 131 were located in the α_2 helix and residue 150 in the dimer–dimer interface but very close to the active site Cys^{119}, located in the α_2 helix (Cys^{119}– Lys135) (Fig. 7A). The reduced form of WT had a fully folded α_2 helix, but the α_2 helix of three mutants had a partial unfolding structure (Fig. 7B–D). Mutant S127C, which had the highest chaperone activity, was unfolded more completely than the others, which is in accordance with the experimental observation. It is evident that changes in the chaperone activity of 2-Cys Prx A could be induced by unfolding the α_2 helix.

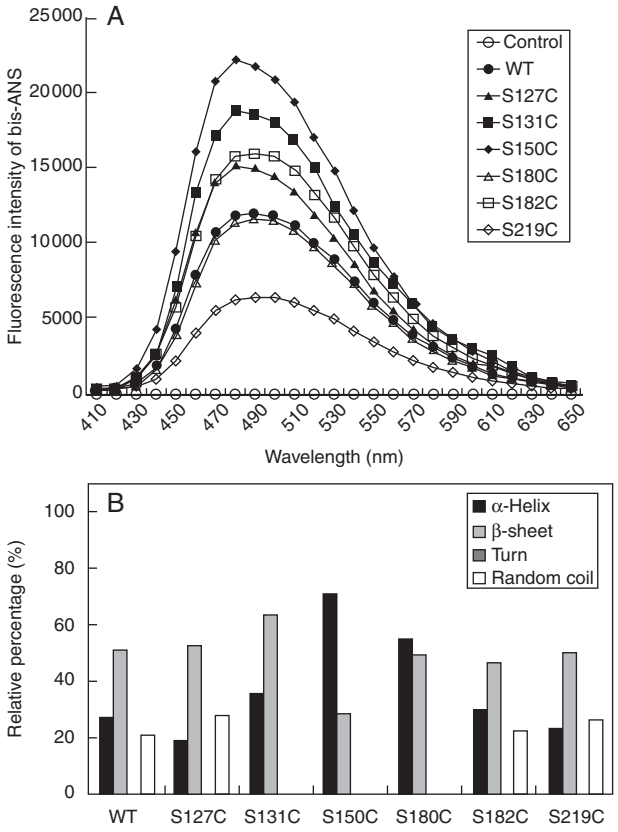

FIG. 5. (A) Changes in hydrophobicity of 2-Cys Prx A and its mutants presented in terms of the fluorescence intensity of bis-ANS. (B) Secondary structure changes of 2-Cys Prx A and its mutant proteins. Black bars, α-helix; grey bars, β-sheet; dark grey bars, turn; white bars, random coil structures.

Earlier research suggested that the peroxidase activity of Prxs can be regulated by the formation of reduced decamer (Barranco-Medina *et al.*, 2009). Hence, the α_2 helix and dimer–dimer interface in the decamer were examined for changes in the peroxidase activity of WT and three mutants. The locations of three mutation sites were identified using the 3-D structure of the constructed 2-Cys Prx A. Residues of Ser^{150}, Ser^{180} and Ser^{182} were located in dimer–dimer interface regions (Fig. 8A). In these three mutants (S150C, S180C, and S182C), mutation positions moved closer to the adjacent dimer (Fig. 8B–D), which can easily form a stable reduced decamer to increase peroxidase activity. Mutants S127C and S131C were located away from the dimer–dimer interface. Therefore, it can be postulated that the distance between mutation residues in each dimer is related to changes in peroxidase activity. On the other hand, S180C and S182C had a fully folded α_2 helix like that of WT 2-Cys Prx A (Fig. 9) and had high peroxidase and low chaperone activity.

Typical 2-Cys Prxs can regulate H_2O_2-mediated cell signalling. In this process, the Prx is inactivated by the hyperoxidation of an active site of a Cys residue to Cys sulphinic acid. Sulphiredoxin (Srx) can restore peroxidase activity and terminates the signal. Srx binds to the C-termial of Prx (Jönsson *et al.*, 2008), and the C-term of 2-Cys Prx A was therefore studied for peroxidase activity change. A difference was observed in the C-term loop region (Asp^{238}–Pro^{256}) near the C-term helix. The C-term loops of S180C and S182C were more flexible

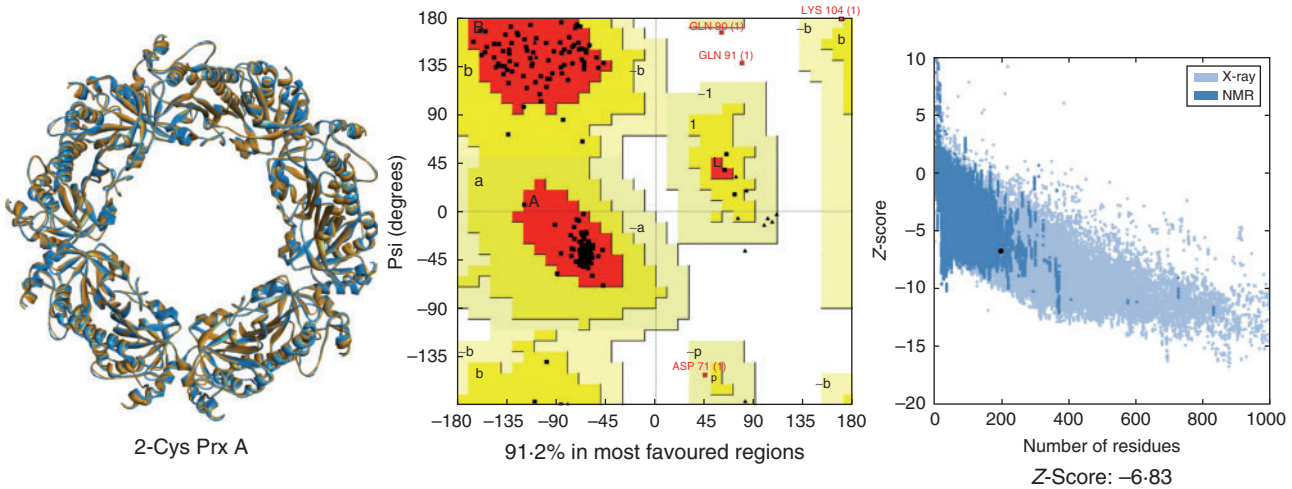

FIG. 6. Homology-modelled structures of 2-Cys Prx A with Ramachandran plot and *Z*-score obtained using the Procheck and ProSA-web programs. Superimposition of the template t HBP23/Prx I (PDB ID: 2Z9S) with the homology-modelled structure of 2-Cys Prx A is shown in the left panel. The structure of the template is coloured blue and the dicameric structure of 2-Cys Prx A is coloured orange. A Ramachandran plot of 2-Cys Prx A obtained by Procheck is shown in the middle panel. A *Z*-score plot of 2-Cys Prx A obtained by ProSA-web is presented in the right panel.

than that of WT. On the contrary, S127C and S131C had a more stable C-term loop than WT. To demonstrate this difference using quantitative data, root mean square fluctuations (RMSF) were calculated for the six systems (except for S219C). In the presence of the inter-disulphide bond, the C-term loop was more flexible than in other cases (Table 1). From the RMSF analysis of the C-term loop region, we clearly observed that the average RMSF values of the regions in the inter-disulphide bond-containing systems (S150C, S180C and S182C) were relatively greater than the values of other systems. This indicates that the inter-disulphide bond made the C-term loop flexible, so that it could easily bind to Srx. Thus, the flexible C-term loop may be a reason for the changes in peroxidase activity of 2-Cys Prx A.

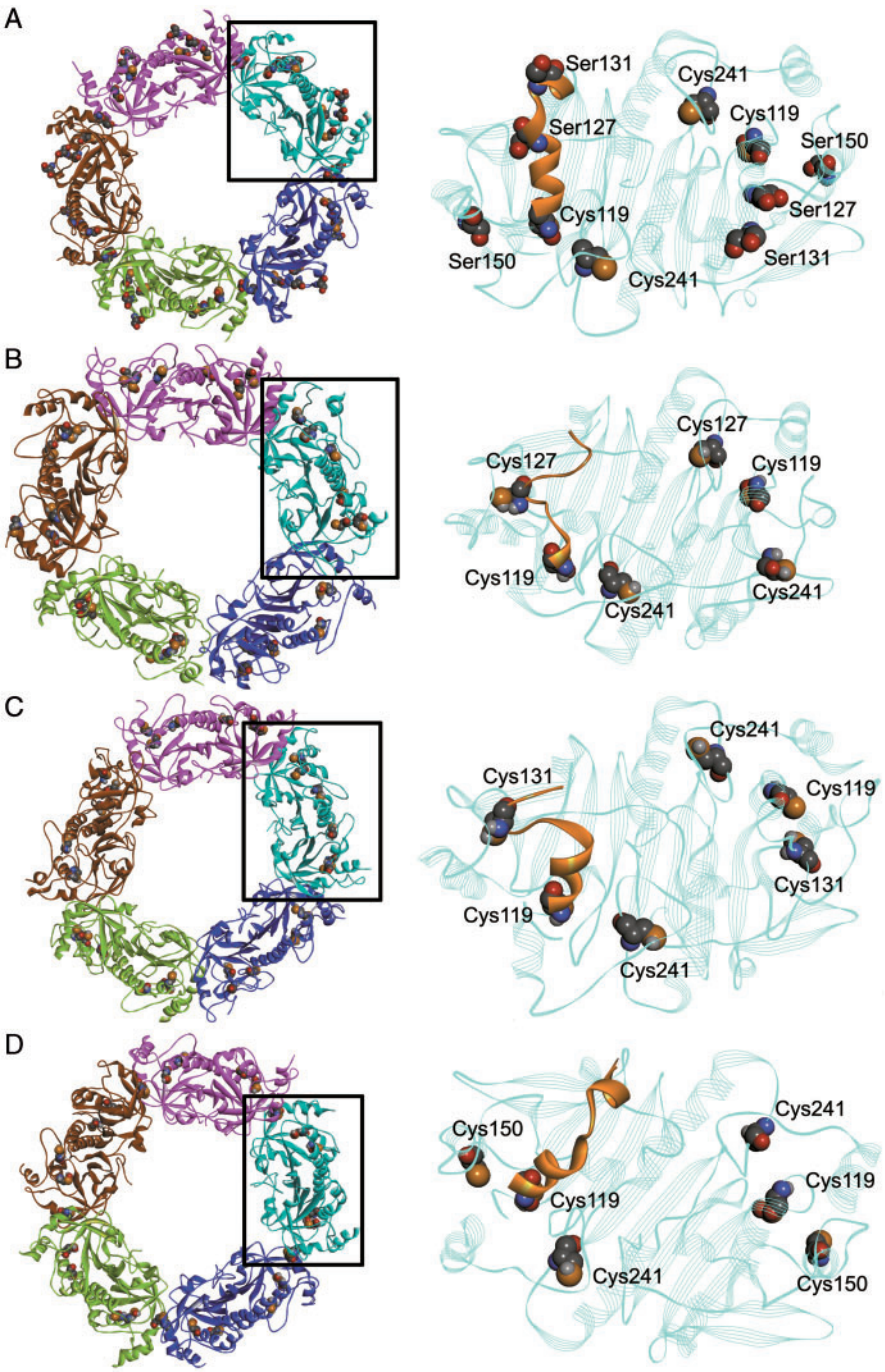

Fig. 7. Decameric structure of four systems showing a change in chaperone activity. Reduced decamer structures of (A) WT 2-Cys Prx A, (B) S127C, (C) S131C and (D) S150C. Detailed views of the dimer region are indicated by squares, showing the catalytic Cys (Cys^{119} and Cys^{241}) and mutation positions marked by CPK style. The α_2 helix is displayed by secondary structure in organ.

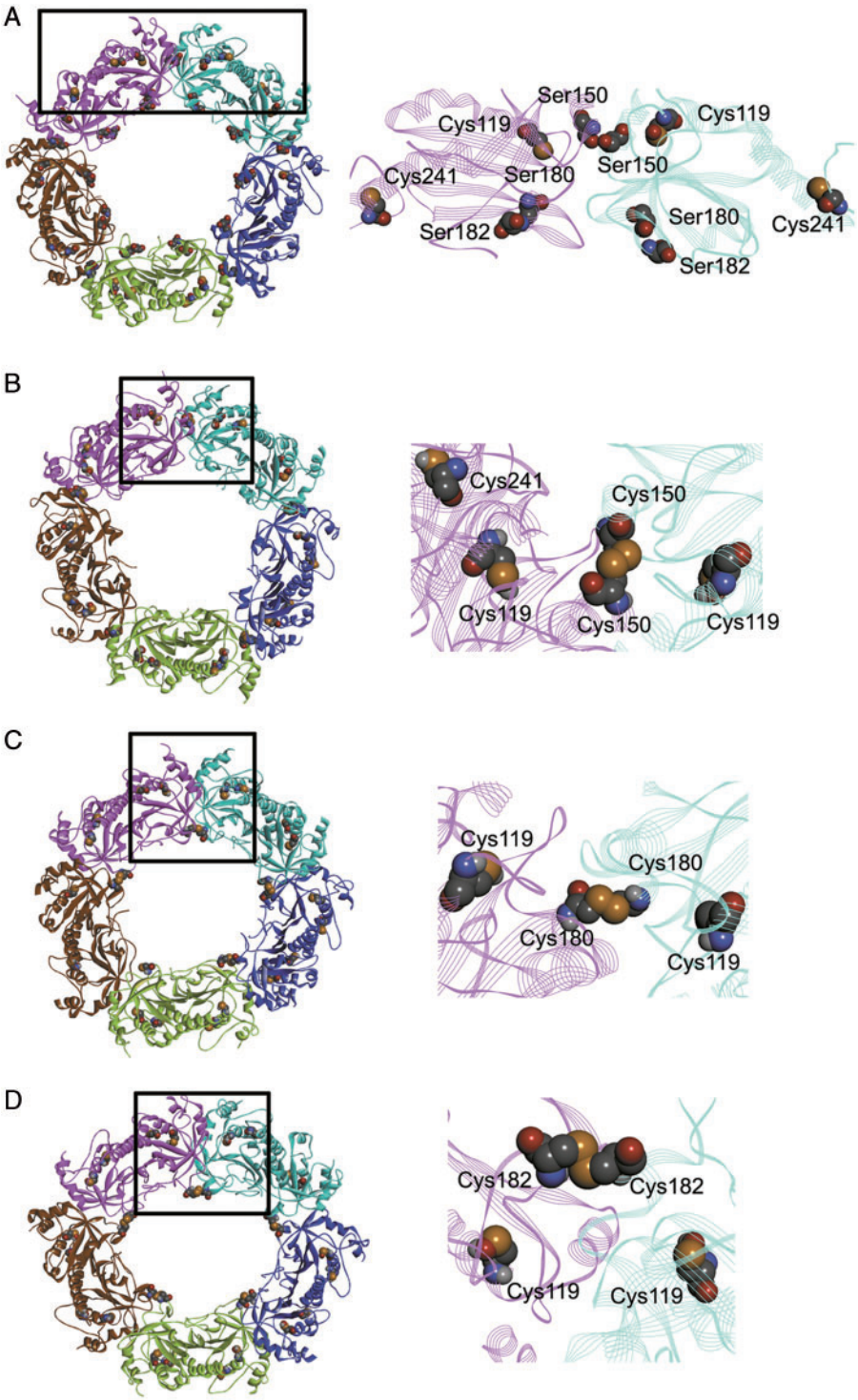

FIG. 8. Decameric structure of four systems showing a change in peroxidase activity. Reduced decamer structures of (A) WT 2-Cys Prx A, (B) S150C, (C) S180C and (D) S182C. Detailed views of the dimer–dimer interface region, indicated by squares, show the catalytic Cys (Cys^{119} and Cys^{241}) and mutation positions represented by CPK style.

DISCUSSION

The 2-Cys Prxs are ubiquitous and highly abundant proteins serving multiple functions in plant cell (Bhatt and Tripathi, 2011). The present study demonstrates the regulation of the dual functions (peroxidase and chaperone) of 2-Cys Prx 2-Cys Prx A through site-targeted replacement of Ser with Cys. For this purpose, a 2-Cys Prx A was identified from *A. thaliana*, cloned, and characterized for its structure and function. *In vitro* enzymatic analysis showed that 2-Cys Prx A, like other 2-Cys Prxs, can perform the dual functions of a Trx-dependent

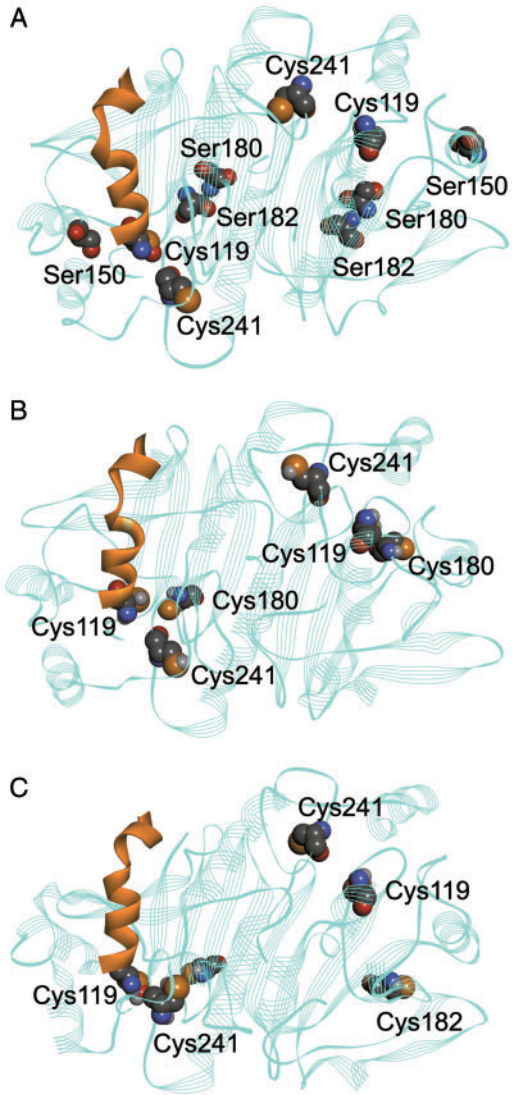

FIG. 9. Dimeric structures of WT, S180C and S182C. Reduced dimers of (A) WT 2-Cys Prx A, (B) S180C and (C) S182C. The catalytic Cys (Cys^{119} and Cys^{241}) and mutation positions are marked by CPK style and the α_2 helix is coloured by organ.

TABLE 1. *Averaged RMSF values of the C-term loop for WT 2-Cys Prx A and six mutants*

Protein	C-term loop (Asp238–Pro256)
WT 2-Cys Prx A	0·140
S127C	0·137
S131C	0·119
S150C	0·157
S180C	0·141
S182C	0·145

peroxidase and a molecular chaperone, which is in good accordance with previous studies (An *et al*., 2011*a*). Based on their observations, An *et al*. (2011*a*) has proposed a model for the functional switching of 2-Cys Prx (PaPrx) based on reversible changes in protein structure. According to this model, 2-Cys Prx can reversibly change its protein structure from HMW complexes to LMW using two different pathways. Furthermore, it was stated that principally 2-Cys Prx exists as oligomers and HMW forms and acts as a chaperone, and subsequently Trx switches most of the HMW complexes to LMW forms to function as Trx-dependent peroxidases, depending on the redox status of the cell (An *et al*., 2011*a*). Purified 2-Cys Prx A also showed discretely sized multiple structures with a diverse range of molecular states, including HMW, LMW and dimeric structures.

2 The functional analysis of fractionated 2-Cys Prx A suggests that chaperone activity was higher than peroxidase activity in spherical-shaped HMW complexes, whereas peroxidase activity was predominant in dimeric forms. The ring-shaped LMW complexes showed dual functions as peroxidase and molecular chaperone. Oligomerization of thiol group proteins is considered to be an important mode of regulation of these dual enzymatic functions. These findings are consistent with earlier reports showing that the dual function of 2-Cys Prx is closely linked with its quaternary structure (König *et al*., 2013).

3 Furthermore, several mutants, *viz*. S127C, S131C, S150C, S180C, S182C and S219C, were generated by site-directed mutagenesis by replacing Ser with Cys in α-helix regions between two active Cys residues of 2-Cys Prx A. These variants formed three types of oligomer under normal conditions, *viz*. HMW complex, LMW complex and dimeric form, with variable proportions. S150C and S180C formed more HMW and LMW complexes than WT, while S180C and S219C predominantly produced dimeric forms. In general, dimeric and HMW forms possess high peroxidase and chaperone activities, respectively while LMW forms have better dual functions (Jang *et al*., 2004; Moon *et al*., 2005). This might be the reason why S150C and S182C, having higher proportions of HMW and LMW forms, showed a significant increase in peroxidase and chaperone activities compared with WT. Similarly, S180C, S182C and S219C showed high peroxidase activity because of their higher proportions of dimeric forms, whereas S127C and S131C showed high chaperone activity due to their HMW forms. Exposure of the hydrophobic domains of a protein is related to its molecular chaperone activity, as to protect target substrates against stress-induced aggregation, chaperones bind to non-native states of protein substrates through these hydrophobic interactions (Ganea, 2001; Jang *et al*., 2006*a*). Replacement of Ser with Cys in the α-helix region of 2-Cys Prx A resulted in an increase in hydrophobicity of most of mutants of could have increased their chaperone activity. However, S150C, having a low dimer peak, showed a different pattern and exhibited higher peroxidase and chaperone activities. In the light of the available data, it is difficult to account exactly for this behaviour of S150C. Residue Ser^{150} (in WT) lies in the dimer–dimer interface region and replacement of Ser with Cys at the 150 position moves it close to an adjacent dimer, which can easily form a stable decamer to increase peroxidase activity. König *et al*. (2013) has also noted variation in function in relation to variation in the conformation of 2-Cys Prx mutants with altered Cys. Further research is required using such mutants to provide detailed understanding of the relation between specific conformational states of 2-Cys Prx A and its function.

4 Molecular evolution has favoured multifunctional 2-Cys Prx proteins switching between peroxidase and chaperone. However, growing interest in the development of an enzyme with enhanced resistance to inactivation and aggregation (König *et al*., 2013) has further necessitated the manipulation in 2-Cys Prxs in order to harness their potential to greatest advantage. Several attempts have already been made to regulate and understand the structure and dual functions of 2-Cys Prx using various methods, including over-oxidation, phosphorylation, chemical modification by methylglyoxal (MGO), heat treatment, gamma radiation, electron beams and Ser → Cys substitution in the α-helix regions between two active Cys residues of a Prx (Rogalla *et al*., 1999; Nagaraj *et al*., 2003; Akhtar *et al*., 2004; Andrew-Aquilina *et al*., 2004; Jang *et al*., 2006*b*; Kanade *et al*., 2009; Lee *at al*., 2009; Park *et al*., 2009; An *et al*., 2011*b*, 2011*c*; Hong *et al*., 2012). However, none of these methods has been shown to be efficient in regulating and enhancing the dual functions of these proteins. The present study has demonstrated that site-directed mutagenesis to replace Ser with Cys at the desired sites between two active Cys residues is an effective means to understand the structure of 2-Cys Prx A (2-Cys Prx) and hence regulate their function.

5 Previous research has demonstrated that the typical 2-Cys Prx adopts four different conformation states, which are related to the switching of its function. Dimers strongly tend to form decamers or dodecamers, while the oxidized form is preferentially present as a dimer. It is a dynamic process. The reduced decamer has strong peroxidase activity, and decamers may associate to produce an HMW form that has chaperone activity (Barranco-Medina *et al*., 2009). Hence, the α_2 helix, dimer–dimer interface and C-term loop have been examined to explain the functional changes (chaperone and peroxidase) of 2-Cys Prx A mutants. Mutants with different activities have shown different structural changes, which are in accordance with previous research. Among seven systems, only S150C showed both chaperone and peroxidase activity, which can be explained by its multiple structural changes. There is strong evidence that activity change of 2-Cys Prx A is not accidental or may unilaterally cause many factors. It is undoubtedly the results. Finally, this modelling study can provide insight into the mechanism by which these mutants change the structure and activity of the protein.

6 A series of molecular modelling approaches was used to understand the mechanism of the 2-Cys Prx A proteins at the molecular level and to trace the reasons why mutants showed altered activities. Seven different models were constructed by homology modelling and then the structures were modified to have sulphenic acid for over-oxidation intermediate state. Subsequently, 10-ns MD simulations were performed to investigate the structure and dynamic behaviour of these models. From the results of MD simulations, it is clear that the activity changes are a result of multiple factors rather than of any single factor. The results of the present modelling study are consistent with our experimental data, and can provide reasonable interpretations and insights for understanding the mechanism of action and the experimental results obtained with 2-Cys Prx A.

7 In conclusion, our work showed that 2-Cys Prx A has dual functions as a peroxidase and as a molecular chaperone. Replacement of Ser^{150} with Cys^{150} (S150C) in the α-helix region of 2-Cys Prx A is an important site for regulating/enhancing dual enzymatic functions. The present findings are mainly based on *in vitro* analyses, but Cys mutagenesis replacing Ser with Cys at amino acid position 150 in the α-helix of 2-Cys Prx A might be a means of developing plants that tolerate various abiotic stresses. *In planta* validation of these findings is the future objective of our research.

ACKNOWLEDGEMENTS

This work was supported by the Nuclear R&D Program of the Ministry of Science, ICT and Future Planning (MSIP), Republic of Korea and the Next-Generation BioGreen 21 Program (PJ01106202) of the Rural Development Administration (RDA) of the Republic of Korea. We gratefully acknowledge Professor Karl-Josef Dietz of Bielefeld University, Germany for his suggestions on the manuscript.

LITERATURE CITED

Akhtar MW, Srinivas V, Raman B, *et al.* 2004. Oligomeric Hsp33 with enhanced chaperone activity. *Journal of Biological Chemistry* **279**: 55760–55769.

An BC, Lee SS, Lee EM, *et al.* 2010. A new antioxidant with dual functions as a peroxidase and chaperone in *Pseudomonas aeruginosa*. *Molecules and Cells*. **29**: 145–151.

An BC, Lee SS, Lee EM, *et al.* 2011a. Functional switching of a novel prokaryotic 2-Cys peroxiredoxin (PpPrx) under oxidative stress. *Cell Stress & Chaperones* **16**: 317–328.

An BC, Lee SS, Lee JT, Hong SH, Wi SG, Chung BY. 2011b. Engineering of 2-Cys peroxiredoxin for enhanced stress-tolerance. *Molecules and Cells* **32**: 257–264.

An BC, Lee SS, Wi SG, Bai HW, Lee SY, Chung BY. 2011c. Improvement of chaperone activity of 2-Cys peroxiredoxin using gamma ray. *Journal of Radiation Research* **52**: 694–700.

Andrew-Aquilina J, Benessch JLP, Ding LL, Yaron O, Horwitz J, Robinson CV. 2004. Phosphorylation of αB-crystallin alters chaperone function through loss of dimeric substructure. *Journal of Biological Chemistry* **279**: 28675–28680.

Baier M, Dietz KJ. 1996. Primary structure and expression of plant homologues of animal and fungal thioredoxin-dependent peroxide reductases and bacterial alkyl hydroperoxide reductases. *Plant Molecular Biology* **31**: 553–564.

Baier M, Dietz KJ. 1997. The plant 2-Cys peroxiredoxin BAS1 is a nuclear-encoded chloroplast protein: its expressional regulation, phylogenetic origin, and implications for its specific physiological function in plants. *Plant Journal* **12**: 179–190.

Baier M, Dietz KJ. 1999. Protective function of chloroplast 2-cysteine peroxiredoxin in photosynthesis: evidence from transgenic *Arabidopsis*. *Plant Physiology* **119**: 1407–1414.

Baier M, Bilger W, Wolf R, Dietz KJ. 1996. Photosynthesis in the basal growing zone of barley leaves. *Photosynthesis Research* **49**: 169–181.

Baier M, Noctor G, Foyer CH, Dietz KJ. 2000. Antisense suppression of 2-Cys peroxiredoxin in *Arabidopsis thaliana* specifically enhance the activities and expression of enzymes associated with ascorbate metabolism but not glutathione metabolism. *Plant Physiology* **124**: 823–832.

Barranco-Medina S, Lázaro JJ, Dietz KJ. 2009. The oligomeric conformation of peroxiredoxins links redox state to function. *FEBS Letters* **583**: 1809–1816.

Berendsen HJC, van der Spoel D, van Drunen R. 1995. GROMACS: a message-passing parallel molecular dynamics implementation. *Computer Physics Communications* **91**: 43–56.

Bhatt I, Tripathi BN. 2011. Plant peroxiredoxins: catalytic mechanisms, functional significance and future perspectives. *Biotechnology Advances* **29**: 850–859.

Burgess SA, Walker ML, Thirumurugan K, Trinick J, Knight PJ. 2004. Use of negative stain and single-particle image processing to explore dynamic properties of flexible macromolecules. *Journal of Structural Biology* **147**: 247–258.

Bussi G, Donadio D, Parrinello M. 2007. Canonical sampling through velocity rescaling. *Journal of Chemical Physics* **126**: 014101.

Chuang MH, Wu MS, Lo WL, Lin JT, Wong CH, Chiou SH. 2006. The antioxidant protein alkylhydroperoxide reductase of *Helicobacter pylori* switches from peroxide reductase to a molecular chaperone function. *Proceedings of National Academy of Sciences of the USA* **103**: 2552–2557.

Darden T, York D, Pedersen L. 1993. Particle mesh Ewald: an N log (N) method for Ewald sums in large systems. *Journal of Chemical Physcis* **98**: 10089.

Dietz KJ. 2003. Plant peroxiredoxins. *Annual Review of Plant Biology* **54**: 93–107.

Dietz KJ. 2011. Peroxiredoxins in plants and cyanobacteria. *Antioxidants and Redox Signalling* **15**: 1129–1159.

Eswar N, Webb B, Marti-Renom MA, *et al.* 2006. Comparative protein structure modeling using modeller. *Current Protocols in Bioinformatics* 5.6. 1–5.6. 30.

Ganea E. 2001. Chaperone-like activity of alpha-crystallin and other small heat shock proteins. *Current Protein and Peptide Science* **2**: 205–255.

Hansen JE, Gafni A. 1993. Thermal switching between enhanced and arrested reactivation of bacterial glucose-6-phosphate dehydrogenase assisted by GroEL in the absence of ATP. *Journal of Biological Chemistry* **268**: 21632–21636.

Hong SH, An BC, Lee SS, *et al.* 2012. Improvement of chaperone activity of 2-Cys peroxiredoxin using electron beam. *Radiation Physics and Chemistry* **81**: 1020–1024.

Jang HH, Lee KO, Chi YH, *et al.* 2004. Two enzymes in one; two yeast peroxiredoxins display oxidative stress-dependent switching from a peroxidase to a molecular chaperone function. *Cell* **117**: 625–635.

Jang HH, Kim SY, Park SK, *et al.* 2006a. Phosphorylation and concomitant structural changes in human 2-Cys peroxiredoxin isotype I differentially regulate its peroxidase and molecular chaperone functions. *FEBS Letters* **580**: 351–355.

Jang HH, Kim SY, Lee SY. 2006b. Oxidative stress-dependent structure and functional regulation of 2-cysteine peroxiredoxins in eukaryotes including plant cells. *Korean Journal of Plant Biotechnology* **33**: 1–9.

Jönsson TJ, Johnson LC, Lowther WT. 2008. Structure of the sulphiredoxin-peroxiredoxin complex reveals an essential repair embrace. *Nature* **451**: 98–101.

Kanade SR, Pasupuleti NR, Nagaraj RH. 2009. Role of cysteine residues in the enhancement of chaperone function in methylglyoxal-modified human αA-crystalline. *Molecular and Cellular Biochemistry* **322**: 185–191.

Kim KH, Alam I, Lee KW, *et al.* 2010. Enhanced tolerance of transgenic tall fescue plants overexpressing 2-Cys peroxiredoxin against methyl viologen and heat stress. *Biotechnology Letters* **32**: 571–576.

Kim MD, Kim YH, Kown SY, *et al.* 2011. Overexpression of 2-Cys peroxiredoxin enhances tolerance to methyl viologen-mediated oxidative stress and high temperature in potato plants. *Plant Physiology Biochemistry* **49**: 891–897.

Kim SY, Jang HH, Lee JR, *et al.* 2009. Oligomerization and chaperone activity of a plant 2-Cys peroxiredoxin in response to oxidative stress. *Plant Science* **177**: 227–232.

Kirchsteiger K, Pulido P, González MC, Cejudo FJ. 2009. NADPH thioredoxin reductase C controls the redox status of chloroplast 2-Cys peroxiredoxins in *Arabidopsis thaliana*. *Molecular Plant* **2**: 298–307.

König J, Galliardt H, Jütte P, Schäper S, Dittmann L, Dietz KJ. 2013. The conformational bases for the two functionalities of 2-cysteine peroxiredoxins as peroxidase and chaperone. *Journal of Experimental Botany* **64**: 3483–3497.

Laskowski RA, MacArthur MW, Moss DS, Thornton JM. 1993. PROCHECK: a program to check the stereo-chemical quality of protein structures. *Journal of Applied Crystallography* **26**: 283–291.

Lee JR, Lee SS, Jang HH, *et al.* 2009. Heat-shock dependent oligomeric status alters the function of a plant-specific thioredoxin-like protein, AtTDX. *Proceedings of the National Academy of Sciences of the USA* **106**: 5978–5983.

Lim JC, Choi HI, Park YS, *et al.* 2008. Irreversible oxidation of the active-site cysteine of peroxiredoxin to cysteine sulfonic acid for enhanced molecular chaperone activity. *Journal of Biological Chemistry* **283**: 28873–28880.

Margreitter C, Petrov D, Zagrovic B. 2013. Vienna-PTM web server: a toolkit for MD simulations of protein post-translational modifications. *Nucleic Acid Research* **41**: w422–w426.

Martí-Renom MA, Stuart AC, Fiser A, Sánchez R, Melo F, Šali A. 2000. Comparative protein structure modeling of genes and genomes. *Annual Review of Biophysics and Biomolecular Structure* **29**: 291–325.

Matsumura T, Okamoto K, Iwahara SI, *et al.* 2008. Dimer-oligomer interconversion of wild-type and mutant rat 2-Cys peroxiredoxin disulfide formation at dimer-dimer interfaces is not essential for decamerization. *Journal of Biological Chemistry* **283**: 284–293.

Moon JC, Hah YS, Kim WY, *et al.* 2005. Oxidative stress-dependent structural and functional switching of a human 2-Cys peroxiredoxin isotype II that enhances HeLa cell resistance to H_2O_2-induced cell death. *Journal of Biological Chemistry* **280**: 28775–28784.

Muthuramalingam M, Siedel T, Laxa M, *et al.* 2009. Multiple redox and non-redox interactions define 2-Cys peroxiredoxin as regulatory hub in the chloroplast. *Molecular Plant* **2**: 1273–1288.

Nagaraj RH, Oya-Ito T, Padayatti PS, *et al.* 2003. Enhancement of chaperone function of α-crystalline by methylglyoxal modification. *Biochemical Journal* **42**: 10746–10755.

Park CH, Lee SS, Kim KR, *et al.* 2014. Optimized enzymatic dual functions of PaPrx protein by proton irradiation. *Journal of Radiation Research* **55**: 17–24.

Park SG, Cha MK, Jeong W, Kim IH. 2000. Distinct physiological functions of thiol peroxidase isoenzymes in *Saccharomyces cerevisiae*. *Journal of Biological Chemistry* **275**: 5723–5732.

Park SK, Jung YJ, Lee JR, *et al.* 2009. Heat-shock and redox-dependent functional switching of an h-type *Arabidopsis* thioredoxin from a disulfide reductase to a molecular chaperone. *Plant Physiology* **150**: 552–561.

Parrinello M, Rahman A. 1981. Polymorphic transitions in single crystals: a new molecular dynamics method. *Journal of Applied Physics* **52**: 7182–7190.

Pulido P, Spinola MC, Kirchsteiger K, *et al.* 2010. Functional analysis of the pathways for 2-Cys peroxiredoxin reduction in *Arabidopsis thaliana* chloroplasts. *Journal of Experimental Botany*. **61**: 4043–4054.

Reed J, Reed TA. 1997. A set of constructed type spectra for the practical estimation of peptide secondary structure from circular dichroism. *Analytical Biochemistry* **254**: 36–40.

Rogalla T, Ehrnsperger M, Preville X, *et al.* 1999. Regulation of Hsp27 oligomerization, chaperone function, and protective activity against oxidative stress/tumor necrosis factor α by phosphorylation. *Journal of Biological Chemistry* **274**: 18947–18956.

Sakamoto A, Tsukamoto S, Yamamoto H, *et al.* 2003. Functional complementation in yeast reveals a protective role of chloroplast 2-Cys peroxiredoxin against reactive nitrogen species. *Plant Journal* **33**: 841–851.

Schmid N, Eichenberger AP, Choutko A, *et al.* 2011. Definition and testing of the GROMOS force-field versions 54A7 and 54B7. *European Biophysics Journal* **40**: 843–856.

Sharma KK, Kaur H, Kumar GS, Kester K. 1998. Interaction of 1,1′-bi(4-anilino)naphthalene-5,5′-disulfonic acid with alpha-crystallin. *Journal of Biological Chemistry* **273**: 8965–8970.

Tripathi BN, Bhatt I, Dietz KJ. 2009. Peroxiredoxins: a less studied component of hydrogen peroxide detoxification in photosynthetic organisms. *Protoplasma* **235**: 3–15.

Van der Spoel D, Lindahl E, Hess B, *et al.* 2010. GROMACS user manual version 4.5. http://www.gromacs.org.

Wiederstein M, Sippl MJ. 2007. ProSA-web: interactive web service for the recognition of errors in three-dimensional structures of proteins. *Nucleic Acid Research* **35**: w407–w410.

Yang KS, Kang SW, Woo HA, *et al.* 2002. Inactivation of human peroxiredoxin I during catalysis as the result of the oxidation of the catalytic site cysteine to cysteine-sulfinic acid. *Journal of Biological Chemistry* **277**: 38029–38036.